Transactions of the **13th International Conference on Structural Mechanics in Reactor Technology** (SMiRT 13), Escola de Engenharia - Universidade Federal do Rio Grande do Sul, Porto Alegre, Brazil, August 13-18, 1995

Crack instability analysis methods of piping systems for LBB applications

Mattar Neto, M.[1], Maneschy, E.[2], Nóbrega, P.G.B.[3]
1) CNEN/SP-IPEN, Comissão Nacional de Energia Nuclear, São Paulo, SP, Brazil
2) FURNAS Centrais Elétricas, São Paulo, SP, Brazil
3) COPESP - Coordenadoria para Projetos Especiais, São Paulo, SP, Brazil

ABSTRACT: The crack instability evaluation is a fundamental step toward confirming the applicability of leak-before-break (LBB) concept in nuclear power plant piping systems. Different approaches have been used to assess stability of cracks: (a) local flow stress (LFS), (b) limit load (LL), (c) elastic-plastic fracture mechanics (EPFM) as J-integral versus tearing modulus (J-T) analysis, and (d) deformation plasticity failure assessment diagram (DPFAD) analysis. The first two approaches are used for high ductile materials, when it is assumed that remaining ligament of the cracked pipe section becomes fully plastic prior to crack extension. EPFM is considered for low ductile piping when the material reaches unstable ductile tearing prior to plastic collapse in the net section. In this paper, the LFS, LL, and EPFM methodologies were applied to calculate failure loads in circumferential through-wall cracked pipes with different materials, geometry configuration, and loadings. This paper presents a comparison among the results obtained from the approaches cited before, and also compares these results with experimental data available in the literature.

1 INTRODUCTION

The instability evaluation of cracked pipes is an estimate commonly used to verify the integrity of high-energy lines of nuclear power plants in a leak-before-break (LBB) program. The systems of a nuclear facility for which LBB is generally applied must be made of ductile materials. Ductile fracture mechanics' methods employ analytical techniques. These analytical techniques extend from elaborate finite element models (FEM) to various elastic-plastic fracture mechanics (EPFM) estimation procedures, such as J-integral versus tearing modulus (J-T), EPRI-NP-6301-D (1989). Also from deformation plasticity failure assessment diagram (DPFAD), EPRI-NP-2431 (1982), to simple limit load (LL), EPRI-NP-6301-D (1989), and local flow stress (LFS), Roos et al. (1989), analyses. FEM analyses are expensive and very time consuming. The purpose of simplified methodologies is to ease the performance of the analyses in terms of time and cost.

LFS is a theory used by Siemens/KWU to conduct LBB evaluation in German nuclear power plants, Bartholomé et al. (1989). LL, in the format presented in the Standard Review Plan 3.6.3 (1987), has been applied in LBB programs in the United States. However, the application of LFS and LL concepts is restricted to high ductile piping

(austenitic wrought and non flux welds) when the material has high resistance to crack propagation. If the ductility is not so high (austenitic flux welds and ferritic materials), the material will reach the unstable tearing stress prior to the limit load. In this case, the applicability of EPFM approaches, such as J-T and DPFAD, may be mandatory.

Although all simplified methods are based on the extent of the theory, it is necessary to include certain idealizing assumptions related to crack shapes, consistent crack geometry, and crack behavior. The crack behavior assumption presupposes that the crack initiates and grows as a result of increasing loads. Also, under most circumstances, it is necessary to obtain other material property data than those of the component being evaluated.

In reality, however, actual flaws may assume complex shapes. For example, the component under evaluation may deform under high loadings, particularly in the vicinity of the flaw (e.g., a pipe may ovalize and its wall may become thinner near the flaw). Also a growing crack may develop shearing lips. These facts together with the inherent variability of the material properties from specimen to specimen lead to a simple and obvious conclusion: perfect correspondence between analytical and experimental results should not be expected at all. On the other hand, to make analytical methods always useful, such methods should be able to predict results within an acceptable uncertainty band which can then be accounted for by appropriate margins.

In this paper, evaluations of circumferential through-wall cracked pipes, using the simplified methods mentioned above, are performed. An in-house computer code was developed to conduct the assessment of crack stability. The results obtained from LFS, LL, J-T, and DPFAD analyses are also compared with experimental data available in the literature. At the end of the paper, some comments and conclusions are addressed based on the comparison of results .

2 LOCAL FLOW STRESS AND LIMIT LOAD CONCEPT

According to LFS or LL concepts, a circumferential through-wall crack in high ductile piping will fail by plastic collapse. In such a case, the flawed structure can be evaluated on the basis of the material strength rather than fracture mechanics. It means that the limit stress or moment at the cracked section are computed only by equilibrium considerations.

If the LFS approach as stated in Roos et al. (1989) is considered, the failure is assumed to occur when the effective stress S_{eff}, at one single point, reaches flow stress. In this case one can write that:

$$(1) \quad S_{eff} = k_a P_m + k_b P_b \leq S_f$$

where P_m is the membrane stress due to axial loadings (pressure plus external loads), P_b is the bending stress due to the external moment, and S_f is the material flow stress (usually assumed as the average value of the yield stress S_y and the ultimate stress S_u). In equation (1), k_a and k_b are the membrane and bending stress magnification factors, and can be defined as:

$$(2a) \quad k_a = \frac{1-\left(\frac{\theta}{\pi}+\frac{\sin 2\theta}{2\pi}-\frac{2\sin\theta}{\pi}\right)}{\left(1-\frac{\theta}{\pi}\right)\left[1-\left(\frac{\theta}{\pi}+\frac{\sin 2\theta}{2\pi}\right)\right]-\frac{2\sin^2\theta}{\pi^2}}$$

$$(2b) \quad k_b = \frac{\frac{\sin\theta}{\pi}\left(1-\frac{\theta}{\pi}\right)}{\left(1-\frac{\theta}{\pi}\right)\left[1-\left(\frac{\theta}{\pi}+\frac{\sin 2\theta}{2\pi}\right)\right]-\frac{2\sin^2\theta}{\pi^2}}$$

where θ is the crack opening half angle as shown in Figure 1.

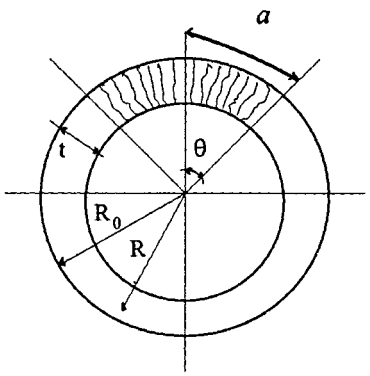

Figure 1. Cracked pipe geometry

For the global instability of the circumferential through-wall crack, the concept for LL is stated in EPRI-NP-6301-D (1989). According to the LL concept, the net section of pipe is assumed to have been completely under plastic yielding. Note that, if the pipe external radius is R_0 and the pipe thickness is t, as shown in Figure 1, and θ is as defined previously, the limit moment M_L to predict the failure may be obtained using the following equation:

$$(3) \quad M_L = 4S_f R_0^2 t\left(1-\zeta+\frac{\zeta^2}{3}\right)(\cos\gamma - 0.5\sin\theta)$$

where:

$$(3a) \quad \zeta = \frac{t}{R_0}$$

$$\gamma = \frac{0.5\theta(1-\zeta)\left(\frac{1+0.5\zeta}{1-\zeta}\right)}{(1-0.5\zeta)} + \frac{P}{\left[4S_f R_0 t(1-\zeta)\right]} \quad (3b)$$

3 EPFM J-T ANALYSIS

The EPFM is based on the concept of J-integral. The parameter J is employed to characterize the crack initiation and extension in ductile materials. The circumferential through-wall crack instability in pipes is predicted by J-T analysis, an approach presented in EPRI-NP-6301-D (1989). According to this reference, from the J-resistance curve obtained from fracture specimens tests (relationship between J and crack extension Δa), it is possible to compute the J-T curve for the material. The crack driving force in terms of the applied parameter J and the tearing modulus T is calculated for the initial crack length as a function of the loading. The intersection of this curve and the J-T curve, for the appropriate material, gives away the instability value of J, defined as J_{inst}. The value of J_{inst}, in a plot of the parameter J versus the load, provides the associated instability load value.

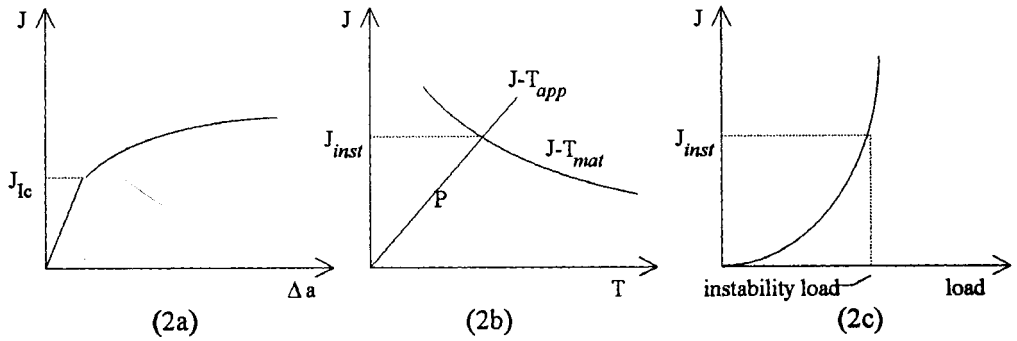

Figure 2 - Crack instability evaluation (J-T analysis procedure)

The J-T analysis procedure, represented in Figure 2, can be detailed as following. From the J-resistance curve for the material, showed in Figure 2a, it is possible to find a correlation between J_{mat} and Δa as expressed in the equation below:

$$J_{mat} = c\,\Delta a^m \quad (4)$$

where c and m are curve fitting constants which are determined in an empirical way. From Figure 2a, it is possible to get the J-integral at the initiation of the crack growth, J_{Ic}. In addition, the material tearing modulus as a function of Δa can be defined as:

$$(5) \qquad T_{mat} = \frac{dJ}{da}\frac{E}{S_f^2}$$

where E is the Young's modulus, and S_f is the flow stress. For the appropriated material, the plot of J-T assumes the shape shown in Figure 2b.

The J-T curve, for the applied loads in piping with through-wall crack, can be computed from the parameter J expressed in the following form:

$$(6) \qquad J_{app}(a) = J_e(a) + J_p(a)$$

In Equation (6), $J_e(a)$ and $J_p(a)$ are the J-integral in the elastic and plastic regimes, respectively. They are available in EPRI-NP-6301-D (1989). These values are functions of the loadings (axial and/or moment), the crack dimension $(\theta = a/R)$, the pipe geometry parameter (R/t), and also the material properties from stress-strain curve (E, S_y, Ramberg-Osgood parameters).

The applied tearing modulus T_{app} is evaluated with Equation (5) with dJ calculated from equation (6), as the variation of the computed $J_{app}(a)$ and $J_{app}(a+\Delta a)$. For small crack growth the applied J-T curve is a straight line. Such line is obtained connecting the origin of the J and T axis with the point P defined by (J_{app}, T_{app}). As illustrated in Figure 2b, the parameter J, at instability of the crack, is identified as J_{inst}. The value of J_{inst} may be obtained from the intersection of the J-T curve, for the material, and the pertinent straight line representing the applied J-T.

The load at instability corresponding to J_{inst} can be evaluated from Figure 2c which is a plot of $J_{app}(a)$ as a function of normalized applied load.

4 EPFM DPFAD ANALYSIS

The DPFAD analysis is applied to define the failure mode associated with the application of specific loadings, flaw size, and piping geometry configuration. It is based on the concept of J-integral. It reveals the instability of cracked pipes undergoing ductile tearing and also whether the failure mode is brittle or if the net section is under plastic collapse.

The diagram defines the safe/fail regions on the S_r-K_r plane. The abscissa S_r is the ratio between the applied stress σ_{app} and the net-section collapse stress σ_b, The ordinate K_r is the ratio between the elastic J-integral, $J_e(a)$, and the applied J-integral, $J_{app}(a)$.

The DPFAD method is illustrated in Figure 3 where the curve is called the failure assessment curve and represents the resistance of the material to failure. The straight line extending from the origin to the assessment point represents the potential for failure. To construct the assessment curve, K_r and S_r are defined as

$$(7) \qquad K_r = \{ J_e(a)/[J_e(a) + J_p(a)]\}^{1/2}$$

$$(8) \qquad S_r = \sigma_{app} / \sigma_b$$

A plot of Equations (7) and (8) on S_r-K_r space defines the failure assessment curve. The region below this curve defines the safe region. The reference net section collapse stress, called σ_b, is obtained from EPRI-NP-6301-D (1989) as a function of the load type, flaw size, shape, and orientation, and also material strength properties. The vertical line in the end of the assessment curve is due to the limit of the maximum allowable applied stress. Remember that the numerator in S_r is the flow stress S_f.

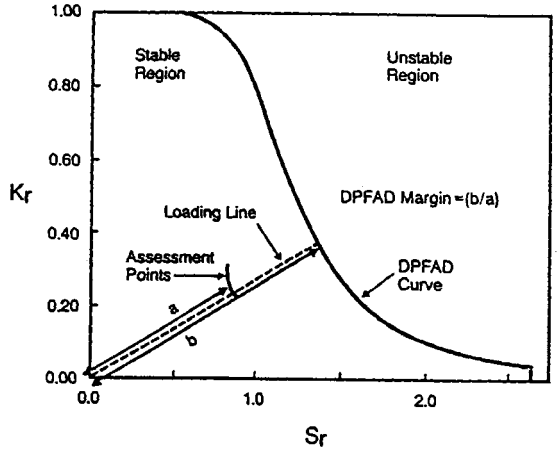

Figure 3. DPFAD diagram

The determination of whether a crack is in the safe region or not can be confirmed from the assessment parameters calculated for specific combination of the applied loading, piping geometry, and crack size. The assessment parameters are defined below and they incorporate crack growth, if needed, in the analysis

(9) $$K_r(a+\Delta a) = \{ J_e(a+\Delta a)/[J_{mat}(a+\Delta a)]\}^{1/2}$$

(10) $$S_r(a+\Delta a) = \sigma_{app} / \sigma_b(a+\Delta a)$$

Once the DPFAD curve has been obtained and the assessment points determined, then the safe/fail margins are based on the distance that the assessment points are from the DPFAD curve.

According to Figure 3, a loading line generated through the origin and an appropriate assessment point intersects the DPFAD curve. For initiation, the appropriate assessment point is determined when J_{mat} equals J_{IC}. For instability, the appropriate assessment point is where the slope of the locus of assessment points equals the slope of the DPFAD curve.

5 RESULTS

Tests are performed in order to assess the integrity of cracked pipes and validate the analysis methods. In Brazil, all the experimental data are referred to J-resistance curve

evaluation and, at the moment, the results from the integrity tests are not yet available. Therefore, the approaches considered in this work to evaluate crack stability will be compared with the results from tests conducted in other countries and available in the literature.

Before presenting the results, it is important to notice that some information were inferred so that the material properties and the parameters required to perform the analyses were acquired. The reason for that is that, unfortunately, some data were not available in the test references. The material data information source used in this paper were (1) EPRI-NP-6301-D (1989), (2) Robert L. Cloud & Associates, Inc. (1992), and (3) Bartholomé et al. (1983). In order to infer the material properties and corresponding parameters, some recommendations of NUREG-1061 (1984) are followed. They are summarized as:

a.) range of stress-strain curve that must be fitted to ensure proper results will vary with pipe and crack geometries. To define appropriate Ramberg-Osgood parameters, it was determined that strains of 1 percent and less comprised the region of interest for the ferritic steel pipe tests, while the appropriate strain for the stainless steel pipe test condition ranged from about 2 to 8 percent;

b.) material resistance to ductile crack extension should be based on a reasonable lower-bound estimation of the material J-resistance curve;

c.) fracture toughness specimens having approximately the same thickness as the pipe wall, and without side grooves, tend to model actual pipe behavior most accurately;

d.) J-integral computational method has certain limits of applicability. Limitations are related to certain assumptions regarding the stress-strain conditions in the region near the crack tip. It is necessary to extrapolate the J-resistance curve in J-T space when those limitations are exceeded.

The results from the methodologies LFS, LL, J-T, and DPFAD were examined on the light of the available experimental data. This was done considering the pipes with circumferential through-wall cracks under internal pressure, bending moment, and also internal pressure plus bending moment together. The comparison between analytical versus experimental initiation and instability loads is showed in Table 1 (internal pressure), Table 2 (bending moment), and Table 3 (internal pressure plus bending moment).

6 CONCLUSIONS AND COMMENTS

All the methods used in this paper are "engineering approaches" based on fracture mechanics with assumptions related to crack shape, consistent geometry, crack behavior, load types and load combinations, material properties and parameters. In some cases, there was a good consistency between the analytical results and the experimental ones. In other cases, the harmony was not so good. The consistencies might be function of the adjustment of some parameters and hypotheses adopted.

In general, the results show that analytical methods give initiation and instability loads smaller than the experimental methods. There is a good agreement between analytical and experimental results where the material properties and the parameters are defined in a more accurate way. It is meaningful to emphasize that material data used in the analyses have different reliability according to what was necessary to estimate for the inputs to evaluate the material data. For example, NUREG 1061 (1984) has almost all

material data necessary to perform the analyses and, in consequence, the analysis results related to those tests are more precise and reliable.

The experimental data tests should be used carefully. For example, the tests K1 and K3 of Table 1 (from the reference Kastner et al. (1981)) present equal experimental instability pressures for pipes with the same geometrical and material characteristics. On the other side, the initial crack lengths are completely different.

The results from J-T and DPFAD analyses are almost equal because similar formulation for J-integral was used for both approaches with the same material data.

The instability loads obtained from J-T, DPFAD and LL analyses are, in general, greater than those obtained from LFS methodology. Apart the difficulties in J-T and DPFAD analyses to define the material properties and parameters, these analyses enable more appropriate conditions to evaluate the behavior of piping systems. This happens because the methods allow to follow the crack growth from the beginning of crack growth up to the crack instability.

The LFS and LL methods, although simpler in terms of formulation and material properties input, ended up in good agreement with experimental results for materials with high ductility. This was observed in Mattar Neto et al. (1994). But such methods may give instability loads values much greater than the experimental ones. This is the case where they are not fully appropriate, mainly with materials with low ductility.

REFERENCES

Bartholomé, G., W. Kastner, E. Klein & R. Wellein, 1983. Ruling-out of fractures in pressure boundary pipings. Part 2. Application to the primary coolant piping. *Reliability of reactor pressure components*: 237-254. Vienna:IAEA.

Bartholomé, G., R. W. Bieselt & M. Erve, 1989. LBB for KWU-plants. *Nuclear Engineering and Design* 111: 3-10.

EPRI-NP-2431, 1982. *A procedure for the assessment of the integrity of nuclear pressure vessels and piping containing defects*. Palo Alto, CA, USA: EPRI

EPRI-NP-6301-D, 1989. *Ductile fracture handbook - Vol. 1 - Circumferential through-wall cracks*. Palo Alto , CA, USA: EPRI

Kastner W., E. Röhrich, W. Schmidt &R. Steinbuch, 1981. Critical crack sizes in ductile piping. *International Journal on Pressure Vessels & Piping* 9: 197-219.

Le Dellion, P. & D. Crouzet, 1990. Experimental and numerical study of circumferentially through-wall cracked pipe under bending including ductile crack growth ovalization. *Fracture, degradation, and fracture - 1990*: 85-92. New York: ASME

Mattar Neto, M., J. E. A. Maneschy & P. G. B. da Nóbrega, 1994. Instability evaluation in austenitic piping systems using two different approaches. *Fatigue, flaw evaluation and leak-before-break assessments*: 299-302. New York: ASME.

NUREG 1061, 1984. *Evaluation of potential for pipe breaks, Vol.3.* Washington, DC: United States Nuclear Regulatory Commission.

Robert L. Cloud & Associates, Inc., 1992. *A specialized course in leak-before-break (LBB) for piping and pressure vessels*. São Paulo, Brazil: RLCA.

Ross, E., K.-H. Herter, P. Julish, G. Bartholomé & G. Senski, 1989. Assessment of large scale pipe tests by fracture mechanics approximation procedures with regard to leak-before-break. *Nuclear Engineering and Design* 112: 183-195.

Standard Review Plan 3.6.3, 1987. *Leak-before-break evaluation procedures*. Section 10.1, Federal Register / Vol.52#167, (for public comment).

Sturm, D., W. Stoppler, K. Hippelein, J. Schiedermaier & H. Zhu, 1987. Experimental investigations on the strength and fracture behaviour of circumferentially cracked piping under internal pressure and outer bending loading. *Design and analysis of piping, pressure vessels and components*: 73-81. New York: ASME.

Table 1. Analytical versus experimental results. Through-wall circumferential cracked pipes under internal pressure

Tests	K1	K2	K3	K4	K5	K6	K7
D_0 (in)	6.98	29.85	6.98	29.85	4.3	4.3	27.72
t (in)	0.429	0.323	0.429	0.327	0.327	0.315	1.496
Material	A106B	Carbon St	A106B	Carbon St	10CrMoNiNh	10CrMoNiNh	20MnMoNi55
Angle (2θ)	34°	42°	68°	76°	156°	200°	190°
P_{Exp} (ksi)	12.79	1.91	12.79	1.78	3.63	1.99	3.15
P_{J-T} / P_{Exp}	1.30	0.75	0.95	0.58	1.71	1.18	0.73
P_{DPFAD} / P_{Exp}	1.29	0.75	0.95	0.57	1.72	1.18	0.73
P_{LL} / P_{Exp}	1.40	1.32	1.09	1.09	1.43	1.20	0.96
P_{LFS} / P_{Exp}	1.25	1.42	0.85	1.30	0.85	0.66	0.88

Tests: K1 to K7 from Kastner et al. (1981)

P_{Exp}: Maximum Experimental Pressure (failure of the pipe)
P_{J-T}: Instability Pressure from J-T analyses
P_{DPFAD} : Instability pressure from DPFAD analyses
P_{LL}: Instability Pressure from LL analyses
P_{LFS}: Instability Pressure from LFS analyses

Table 2. Analytical versus experimental results. Through-wall circumferential cracked pipes under bending moment

Tests	D1	D2	D3	S1	S2	S3	R1	N1	N2	N3
D_0 (in)	16	16	16	31.5	31.5	31.5	27.5	16	4.51	2.375
t (in)	1.6	1.6	1.6	1.85	1.85	1.85	1.858	1.0276	0.354	0.237
Material	SS316	SS316	SS316	20MnMo Ni55	20MnMo Ni55	20MnMo Ni55	bainitic st	SS304	SS304	SS304
Angle (2θ)	120°	40°	40°	60°	60°	20°	60°	132.3°	133.56°	133.56°
MExp Init (lbf in)	5.656E6	1.026E7	9.754E6	-	-	-	8.143E7	6.609E6	1.526E5	2.962E4
MExp Inst (lbf in)	6.665E6	1.250E7	1.191E7	8.541E7	7.877E7	1.231E8	8.541E7	6.957E7	1.576E5	2.996E4
MJ-T Init + MExp Init	0.83	0.89	0.70	-	-	-	0.33	0.76	1.03	1.01
MJ-T Inst + MExp Inst	0.75	0.78	0.63	0.82	0.89	0.81	0.39	0.81	1.05	1.00
MDPFAD Init + MExp Init	0.82	0.90	0.70	-	-	-	0.32	0.77	1.03	1.01
MDPFAD Inst + MExp Inst	0.75	0.79	0.64	0.83	0.89	0.80	0.39	0.81	1.05	1.00
MLL Inst + MExp Inst	0.75	0.70	0.76	0.69	0.75	0.90	0.52	0.79	0.83	0.71
MLFSInst + MExp Inst	0.76	0.44	0.44	0.39	0.42	0.59	0.29	0.48	0.52	0.45

Tests: D1 to D3 from Le Dellion & Crouzet (1990), S1 to S3 from Sturm et al. (1987), R1 from Roos et al. (1989), and N1 to N3 from NUREG-1061 (1984)

MExp Init: Experimental initiation moment
MExp Inst: Experimental maximum moment (failure of the pipe)
MJ-T Init: Initiation moment from J-T analysis
MJ-T Inst: Instability moment from J-T analysis
MDPFAD Init : Initiation moment from DPFAD analysis
MDPFAD Inst: Instability moment from DPFAD analysis
MLL Inst: Instability moment from LL analysis
MLFS Inst: Instability moment from LFS analysis

Table 3: Analytical versus experimental results. Through-wall circumferential cracked pipes under internal pressure plus bending moment

Tests	K8	K9	S4	R2	R3	R4	R5
Do (in)	4.88	4.88	31.5	16.81	16.81	16.	27.5
t (in)	0.337	0.337	1.85	0.63	0.63	0.394	1.858
Material	SS304	SS304	NiCrMo Special Melt	ferritic bainitic St	ferritic bainitic St	ferritic bainitic St	bainitic St
Angle (2θ)	76°	135°	60°	90°	45°	60°	60°
Internal Pressure (psi)	2495	1049	2175	1160	1160	1160	2175
MExp Init (lbf in)	-	-	-	3.717E6	7.966E6	3.664E6	-
MExp Inst (lbf in)	1.221E5	8.348E4	4.868E7	7.028E6	1.133E7	4.903E6	4.868E7
MJ-T Init + MExp Init	-	-	-	0.59	1.11	0.59	-
MJ-T Inst + MExp Inst	0.88	0.80	0.43	0.34	0.79	0.47	0.57
MDPFAD Init + MExp Init	-	-	-	0.59	1.10	0.59	-
MDPFAD Inst + MExp Inst	0.88	0.80	0.44	0.34	0.79	0.47	0.58
MLL Inst + MExp Inst	1.18	0.77	1.15	0.44	0.75	0.82	0.87
MLFS Inst + MExp Inst	0.79	0.85	0.34	0.24	0.35	0.24	0.29

Tests: K8 and K9 from Kastner et al. (1981), S4 from Sturm et al. (1987),and R2 to R5 from Roos et al. (1989)

MExp Init: Experimental initiation moment
MExp Inst: Experimental maximum moment (failure of the pipe)
MJ-T Init: Initiation moment from J-T analysis
MJ-T Inst: Instability moment from J-T analysis
MDPFAD Init: Initiation moment from DPFAD analysis
MDPFAD Inst: Instability moment from DPFAD analysis
MLL Inst: Instability moment from LL analysis
MLFS Inst: Instability moment from LFS analysis